Mathematics

https://www.aimspress.com/journal/Math

AIMS Mathematics, 11(9): 29145–29178.
DOI: 10.3934/math.20261159
Received: 24 June 2026
Revised: 05 August 2026
Accepted: 27 August 2026
Published: 10 September 2026

Research article

Fractional-order adaptive sliding mode containment control of multi-drone systems with unknown time-varying payloads and input constraints

Hanen Louati[1] **and Mohammed M. A. Almazah**[2,*]

[1] Mathematics Department, Faculty of Science, Northern Border University, Arar, KSA, Saudi Arabia; Email: Hanen.Louati@nbu.edu.sa

[2] Department of Mathematics, College of Sciences, King Khalid University, Abha, 61421, Saudi Arabia

* **Correspondence:** Email: mmalmazah@kku.edu.sa.

Abstract: A resilient containment control scheme was developed in this work for a category of fractional-order multi-drone networks, specifically managing the joint effects of mass changes, bounded control inputs, communication lags, component faults, and external disturbances. Unlike conventional unmanned aerial vehicle (UAV) control approaches that assume fixed or known payload parameters, the proposed framework explicitly considers unknown and time-varying payload mass, which significantly affects the dynamic behavior and stability of aerial vehicles during cooperative missions. A novel adaptive containment control protocol was developed by integrating fractional-order sliding mode control with an online payload mass adaptation mechanism, enabling each follower UAV to accurately estimate payload variations in real time. The containment objective was achieved with respect to multiple dynamic leaders under a directed communication topology. Rigorous Lyapunov stability analysis based on fractional-order Mittag–Leffler theory was provided to prove the boundedness of all closed-loop signals and the convergence of containment errors, while maintaining stability despite control input limitations and physical mechanism failures. Furthermore, the proposed control scheme ensures robustness against communication delays and matched disturbances. Extensive numerical simulations involving a 12-UAV formation scenario exhibited the effectiveness and supremacy of the proposed payload-adaptive strategy compared with non-adaptive methods, highlighting significant improvements in containment accuracy, control effort, and system robustness.

Keywords: fractional-order systems; multi-UAV systems; containment control; payload mass adaptation; fault-tolerant control; input saturation; communication delays; sliding mode control
Mathematics Subject Classification: 26A33, 34K37

1. Introduction

Fractional-order fault-tolerant containment control has been widely investigated to enhance the robustness and stability of multi-UAV systems under uncertainties and actuator faults [1]. Payload transportation is one of the most important applications of cooperative UAV systems, where changes in payload mass and inertial properties significantly influence flight stability and control performance. To address these challenges, adaptive nonlinear control strategies have been developed for UAV payload transportation systems to compensate for uncertain payload dynamics and improve tracking accuracy [2]. The design of lifting and transportation mechanisms for collaborative robotic systems has also been investigated to enhance the efficiency and reliability of payload delivery missions [3]. Energy-based adaptive control approaches have demonstrated improved robustness for quadrotor UAVs carrying suspended payloads under nonlinear dynamics and external disturbances [4]. Furthermore, flexible payload transportation systems have been studied by incorporating detailed dynamic models and experimentally validated controllers to ensure stable operation during payload motion [5]. Hierarchical adaptive control frameworks have also been proposed for rotorcraft carrying cable-suspended payloads, showing improved disturbance rejection and trajectory tracking performance under varying payload conditions [6]. Although these studies have made significant progress in payload transportation and adaptive control, they do not simultaneously address fractional-order containment control, actuator faults, input saturation, communication delays, and unknown payload variations in cooperative multi-UAV networks. These limitations motivate the development of the resilient containment control strategy proposed in this paper. To reduce communication burden and improve efficiency, distributed and event-triggered fractional-order fault-tolerant control schemes have been developed for multi-UAV systems with state constraints [7]. Formation control methods combining fuzzy logic and prescribed performance under saturation constraints have been reported to enhance transient behavior [8]. Delay effects on containment performance have been systematically analyzed through delay-margin-based approaches in fractional-order multi-agent systems [9]. Robust multi-object tracking approaches have further improved target association performance in forward-looking sonar applications [10]. Unified aeroelastic and flight dynamics formulations have been developed to improve the modeling accuracy of aerospace systems [11]. Rapid aerodynamic analysis methods have also been proposed by combining panel methods with boundary layer theory for efficient aerodynamic prediction [12].

Adaptive and learning-based fault-tolerant control approaches have gained increasing interest, including adaptive dynamic programming techniques for multi-UAV formations [13]. Recent advances have also been reported in intelligent control and optimization for autonomous systems. Prior-controller-assisted multi-agent deep reinforcement learning has been developed to improve the attitude control performance of hypersonic morphing vehicles under complex flight conditions [14]. Machine learning techniques have also been employed to accelerate the hydrodynamic shape design of autonomous underwater vehicles, thereby improving the design efficiency and prediction accuracy [15]. Robust obstacle avoidance strategies based on reinforcement learning have demonstrated improved navigation performance for unmanned underwater vehicles operating in uncertain environments [16]. Event-triggered tube model predictive control with input-to-state stability guarantees has further enhanced the robustness of vehicle motion control under external disturbances while reducing the computational burden [17].

Neural-network-based aerodynamic parameter prediction methods have been proposed to improve the modeling accuracy of airfoil characteristics [18]. Furthermore, adaptive impedance sliding mode control with stiffness scheduling has been developed to achieve robust trajectory tracking and compliant interaction in rehabilitation robotic systems [19]. Although these studies have achieved significant progress in intelligent control, learning-based optimization, and autonomous system design, they do not address resilient fractional-order containment control of cooperative multi-UAV systems subject to actuator faults, payload uncertainty, communication delays, and input saturation simultaneously. Finite-time fault-tolerant attitude control strategies based on disturbance observers have been shown to improve the convergence speed [20]. Specified-time fault-tolerant tracking control has further strengthened time-performance guarantees in UAV formations [21]. Recent studies have explored various intelligent control and modeling strategies for autonomous systems. Data-driven modeling and control methods considering communication time delays have improved the robustness and dynamic performance of wireless power transfer systems under uncertain operating conditions [22]. Multi-layer dynamic information propagation models have also been developed to describe the evolution of complex networked systems with heterogeneous behavioral characteristics [23].

Anonymous dynamic formation control with obstacle avoidance has enhanced the safety and coordination capability of multi-agent systems operating in uncertain environments [24]. Function-based behavioral modeling approaches have further improved the fidelity and efficiency of air combat simulation for autonomous aerial platforms [25]. Adaptive robust control strategies have been proposed for underactuated robotic systems to achieve accurate constraint-following performance under nonlinear uncertainties [26]. Leakage-type adaptive robust control methods have also demonstrated improved trajectory tracking and parameter adaptation for collaborative robotic systems with fuzzy uncertainties [27]. Furthermore, low-latency brain-computer interface-based robotic navigation has been developed to enhance real-time autonomous mobility and human–robot interaction [28]. Although these studies have significantly advanced intelligent control, modeling, and autonomous system applications, they do not simultaneously address fractional-order containment control, actuator faults, payload uncertainty, communication delays, and input saturation in cooperative multi-UAV systems. Communication rate optimization in multi-UAV relay systems has also been explored [29]. Event-triggered finite-time formation control under input saturation has been developed to improve convergence properties [30].

Recent studies have highlighted system-level challenges and open issues in autonomous multi-UAV coordination [31]. Sun et al. [32] proposed a resilient continuous UAV localization framework that combines cross-view perception with particle filtering to improve localization accuracy in complex environments. Although the method enhances navigation robustness against localization uncertainties, it does not consider fractional-order containment control, actuator faults, communication delays, input saturation, or adaptive payload estimation for cooperative multi-UAV systems. Tang et al. [33] proposed a generative AI-enhanced multi-agent reinforcement learning framework for task assignment and exploration optimization in low-altitude UAV rescue missions. Their approach improves cooperative decision-making and mission efficiency; however, it does not address fault-tolerant containment control, fractional-order dynamics, communication delays, input saturation, or unknown payload variations in multi-UAV systems. Tang et al. [34] proposed a cooperative pursuit strategy for fixed-wing UAVs operating in complex terrain to improve target interception performance while satisfying flight constraints. Their method demonstrated effective cooperative guidance in challenging environments; however, it does not consider actuator faults, communication delays, input saturation, or fractional-order containment control in multi-UAV systems. Recently, Fu et al. [35] developed an adaptive safety attitude control scheme for hybrid vertical take-off and landing (VTOL) UAVs under multiple actuator faults and uncertainties. By integrating adaptive sliding mode control with fault compensation, their method improves tracking performance and robustness during transition flight. However, the proposed approach is limited to the attitude control of a single hybrid VTOL UAV and does not consider fractional-order containment control, communication delays, input saturation, or adaptive payload estimation in cooperative multi-UAV systems.

Distributed containment control for multi-UAV networks has become highly critical for safely guiding follower drones into a dynamic convex hull spanned by multiple leaders. While fractional-order calculus effectively captures the hereditary memory and viscoelastic aerodynamic effects inherent in complex flight dynamics, maintaining containment tracking precision remains challenging under actuator anomalies, input saturation, communication latencies, and online payload mass fluctuations. Recent literature has explored cooperative tracking under specialized operational constraints, such as output formation containment for time-delayed singular systems with stochastic impulses [36], robust bipartite containment under malicious false data injection attacks using zero-sum games [37], and fractional-order singular consensus utilizing adaptive pinning laws over switching topologies [38]. Recent advances have also investigated the performance analysis of multiple-input multiple-output (MIMO) information systems under communication delays and message queue effects, demonstrating the significant influence of network-induced delays on system stability and performance [39]. These studies provide valuable insights into delay-dependent system analysis. However, unlike information network systems, the present work focuses on fractional-order multi-UAV containment control with unknown payload variations, actuator faults, and input saturation under delayed inter-UAV communication.

Recent studies have also investigated predefined-time formation control for multi-agent systems under complex communication and security constraints. Predefined-time synchronized bipartite formation control has been developed for networked heterogeneous Euler–Lagrange systems, providing guaranteed convergence within a prescribed time despite heterogeneous agent dynamics [40]. In addition, predefined-time sliding-mode formation control has been proposed for second-order nonlinear multi-agent systems under deception attacks, demonstrating improved resilience against malicious network-induced disturbances while maintaining formation accuracy [41]. Although these approaches provide valuable advances in predefined-time coordination and secure formation control, they do not simultaneously consider fractional-order UAV dynamics, unknown payload variations, actuator faults, input saturation, and communication delays. These challenges motivate the development of the proposed adaptive fractional-order containment control framework.

Recent studies have explored hybrid modeling techniques to improve the prediction accuracy of nonlinear vehicle dynamics under limited driving data [42]. Time-synchronized control strategies have also been developed to enhance the tracking performance of constrained nonlinear systems [43]. Hybrid neural network and physics-based estimation methods have further improved longitudinal vehicle dynamics modeling with limited data availability [44]. Distributed safety-critical formation control has been investigated using bearing estimators and control barrier functions to ensure collision-free cooperative operation [45]. Robust adaptive dynamic programming has been proposed to improve the control performance of hypersonic vehicles under unmatched uncertainties [46]. Segmented activation function-based zeroing neural network methods have demonstrated efficient solutions for dynamic equations and robotic manipulator control [47]. Adaptive sliding mode control combined with randomized neural networks has also been applied to uncertain tilting quadrotor systems to improve robustness against uncertainties [48]. Sliding mode observer design has been investigated for descriptor systems with limited observability to enhance state estimation performance [49]. Adaptive fuzzy control strategies have achieved predefined-time convergence and improved tracking accuracy for nonlinear systems [50]. Observer-based adaptive fuzzy fractional backstepping control has further enhanced consensus performance of uncertain multi-agent systems under event-triggered communication [51]. Minimum operator-based data-driven sliding mode control has been developed to improve the performance of magnetorheological fluid dual-clutch systems [52]. Modified super-twisting sliding mode control has been introduced to improve braking performance of aircraft systems under disturbances and parameter uncertainties [53]. Adaptive anti-skid braking control methods have also been proposed to compensate for runway disturbances and improve braking stability [54]. Inverse reinforcement learning has been employed to develop inverse optimal tracking control for AC/DC converter systems [55]. Human digital twin-assisted motion planning has been explored to improve the safety of industrial human–robot interaction [56]. Although these studies have advanced intelligent modeling, adaptive control, and autonomous system design, they do not simultaneously address fractional-order containment control, actuator faults, unknown payload variations, communication delays, and input saturation in cooperative multi-UAV systems. Therefore, this paper develops a unified resilient containment control framework to address these challenges.

However, a framework that simultaneously tackles the coupled challenges of fractional dynamics, non-smooth input saturation, and online payload variations within a fault-tolerant multi-UAV containment scheme has not yet been established. To bridge this gap, this paper constructs a payload-aware distributed adaptive containment architecture. Distributed containment control has become an important research topic for cooperative multi-UAV systems operating in uncertain environments. Recent studies have investigated fractional-order containment control under actuator faults, event-triggered communication, communication delays, and external disturbances. Other works have addressed specific challenges such as adaptive fault-tolerant control, robust formation tracking, and containment under cyber attacks or stochastic disturbances. Although these contributions have significantly advanced the field, most existing methods assume fixed vehicle parameters or do not explicitly account for unknown and time-varying payload mass during flight.

In practical missions, payload variations modify the total vehicle mass and influence the system dynamics, resulting in degraded tracking accuracy and reduced control performance if they are not properly compensated. Furthermore, only limited attention has been given to integrating payload adaptation with fractional-order sliding mode containment control while simultaneously considering actuator faults, input saturation, and communication delays. Motivated by these limitations, this paper develops a distributed adaptive containment control framework that combines online payload mass estimation with fractional-order sliding mode control to enhance robustness and maintain accurate containment performance under multiple practical constraints. Unlike existing containment control approaches that address only one or a few practical challenges, the proposed framework simultaneously considers fractional-order UAV dynamics, unknown payload variations, actuator faults, input saturation, communication delays, and external disturbances within a unified control

architecture. The main novelty of this work is not the use of each individual technique, but their systematic integration into a resilient adaptive containment control framework in which the adaptive payload estimator, fractional-order sliding mode controller, and neural-network-based uncertainty approximator operate cooperatively. This unified design improves robustness, tracking accuracy, and containment performance under multiple practical uncertainties while maintaining theoretical stability guarantees. This is how the content is organized:
Section 1: This section motivates the study by highlighting the limitations of existing multi-UAV containment control approaches when payload variations, actuator faults, input saturation, and communication delays coexist. The necessity of incorporating payload awareness into fractional-order fault-tolerant containment control is emphasized, and the main objectives and novelties of the proposed work are outlined.
Section 2: This section formulates a payload-aware fractional-order multi-UAV system model that explicitly accounts for actuator faults, input saturation, and communication delays. Fundamental concepts related to fractional calculus, graph theory, containment control, and system admissibility are introduced to demonstrate the theoretical foundation for subsequent analysis.
Section 3: In this section, the fault-tolerant containment control problem is rigorously defined for payload-varying fractional-order multi-UAV systems. The control objectives, fault models, saturation constraints, and delay effects are mathematically characterized, providing a clear and unified problem statement.
Section 4: This section presents the design of a distributed payload-aware fractional-order fault-tolerant containment controller. An adaptive mechanism is introduced to compensate for unknown payload variations and actuator faults, while saturation nonlinearities and communication delays are explicitly handled within the control framework.
Section 5: This section develops a fractional-order Lyapunov-based stability analysis to rigorously prove admissibility, boundedness, and containment convergence of the closed-loop system. Sufficient conditions are derived to guarantee robust containment performance despite payload uncertainty, faults, input saturation, and delays.
Section 6: This section provides comprehensive numerical simulations involving multiple UAVs to validate the effectiveness of the proposed control scheme. Comparative results demonstrate improved containment accuracy, reduced control effort, and enhanced robustness against faults and payload variations.
Section 7: This section summarizes the main findings and contributions of the paper. The advantages of the proposed payload-aware fractional-order fault-tolerant containment control approach are highlighted, and potential directions for future research are discussed.

Paper contributions

The paper has made the following key contributions to this research:

- A novel payload-aware fractional-order multi-UAV system model is developed that simultaneously considers actuator faults, input saturation, and communication delays, capturing key practical challenges in real-world UAV operations.
- A distributed adaptive fault-tolerant containment control scheme is proposed, incorporating an online payload mass adaptation mechanism to effectively compensate for unknown and time-

varying payload uncertainties.

- The designed control framework explicitly addresses actuator fault effects and input saturation constraints, ensuring robustness and feasibility under hardware and operational limitations.
- Comprehensive numerical simulations and comparative studies are presented to validate the effectiveness, robustness, and reduced control effort of the proposed control scheme under multiple challenging scenarios.

2. Problem formulation with payload dynamics

2.1. UAV model with payload

Consider a group of N fractional-order UAVs consisting of a set of followers $\mathcal{F} = \{1, 2, \ldots, N_f\}$ and a set of leaders $\mathcal{L} = \{N_f + 1, \ldots, N\}$. Each UAV is assumed to carry a rigid payload rigidly attached to its body. Let m_u and m_p denote the mass of the UAV and the payload, respectively. Then, the total mass of the ith UAV is given by

$$m_i = m_u + m_{p,i}. \tag{2.1}$$

The fractional-order translational dynamics of the ith UAV with payload are described as

$$D^\alpha x_i(t) = v_i(t), \tag{2.2}$$

$$m_i D^\alpha v_i(t) = u_i(t) - m_i g e_3 + d_i(t) - \Delta_i(t), \tag{2.3}$$

where $x_i(t) \in \mathbb{R}^3$ and $v_i(t) \in \mathbb{R}^3$ denote the position and velocity vectors, $u_i(t) \in \mathbb{R}^3$ is the control input, g is the gravitational constant, $e_3 = [0, 0, 1]^T$, $d_i(t)$ represents external disturbances, $\Delta_i(t)$ denotes the lumped payload-induced uncertainty. The payload uncertainty term $\Delta_i(t)$ includes the effects of payload mass variation, aerodynamic coupling, payload-induced drag, and is assumed to be unknown but bounded. Dividing (2.3) by m_i, this model can be reformulated into the following state-space representation:

$$D^\alpha v_i(t) = \frac{1}{m_i} u_i(t) - g e_3 + F_i(x_i, v_i), \tag{2.4}$$

where $F_i(x_i, v_i)$ represents the lumped uncertainty caused by payload variation and disturbances.

2.2. Actuator faults and input saturation

Every drone within the fleet is constrained by actuator saturation and vulnerability to defects. The operational model for a compromised actuator is defined as follows:

$$u_i(t) = \mathrm{sat}(G_i u_{ci}(t) + f_i(t)),$$

where $u_{ci}(t)$ is the designed control signal, $G_i = \mathrm{diag}(g_{i1}, g_{i2}, g_{i3})$ is the actuator effectiveness matrix with $0 < g_{ij} \le 1$, $f_i(t)$ denotes actuator bias faults,and $\mathrm{sat}(\cdot)$ represents the actuator saturation nonlinearity. Substituting the faulty actuator model into (2.4), the closed-loop dynamics become

$$D^\alpha v_i = \frac{1}{m_i} \mathrm{sat}(G_i u_{ci} + f_i) - g e_3 + F_i(x_i, v_i). \tag{2.5}$$

It should be emphasized that the proposed containment controller is developed for the translational motion of the quadrotor. The rotational (attitude) dynamics are introduced only to describe the complete physical model and to provide the relationship between the generated thrust and translational motion. Consequently, the controller design, adaptive laws, and stability analysis are established using the translational dynamics given in Eqs (2.2)–(2.5), whereas the attitude subsystem is assumed to be stabilized by a low-level flight controller operating independently.

2.3. Communication topology and delays

The communication topology of the UAV network is represented by the directed graph $\mathcal{G} = (\mathcal{V}, \mathcal{E}, \mathcal{A})$, where $\mathcal{V}$, $\mathcal{E}$, and $\mathcal{A}$ denote the node set, edge set, and weighted adjacency matrix, respectively. The transmission of information between neighboring UAVs is subject to communication delays, where τ_{ij} denotes the delay from UAV j to UAV i. To facilitate the subsequent stability analysis, the communication delay is assumed to be bounded according to

$$0 \leq \tau_{ij} \leq \bar{\tau},$$

where $\bar{\tau}$ denotes the maximum admissible delay. The delay is incorporated into the containment error dynamics, while its influence on the closed-loop system is treated as a bounded perturbation. Under Assumption 4.2, the proposed adaptive sliding mode controller compensates for this bounded delay effect and preserves containment performance.

2.4. Containment control objective

The communication topology is described by a directed graph composed of leaders and followers. Let a_{ij} denote the (i, j)th element of the follower–follower adjacency matrix, where $a_{ij} > 0$ if follower j communicates with follower i, and $a_{ij} = 0$ otherwise. Similarly, b_{ik} denotes the (i, k)th element of the leader–follower adjacency matrix, where $b_{ik} > 0$ if leader k directly transmits information to follower i, and $b_{ik} = 0$ otherwise. For each follower UAV $i \in \mathcal{F}$, define the containment error as

$$e_i(t) = \sum_{j \in \mathcal{N}_i} a_{ij}(x_i(t) - x_j(t - \tau_{ij})) - \sum_{k \in \mathcal{L}} b_{ik}(x_i(t) - x_k(t - \tau_{ik})). \tag{2.6}$$

In the considered communication network, information exchanged among neighboring followers and between leaders and followers is subject to transmission delays caused by wireless communication, computation, and network latency. Accordingly, the containment error is formulated by incorporating the communication delays in both follower–follower and leader–follower information exchange. Let τ_{ij} and τ_{ik} denote the communication delays from follower j to follower i and from leader k to follower i, respectively, where $e_i(t)$ denotes the containment error of follower UAV i, $\mathcal{N}_i$ is the set of neighboring followers, and $\mathcal{L}$ represents the set of leader UAVs. The weighting coefficients a_{ij} and b_{ik} characterize the follower–follower and leader–follower communication links, respectively, where $\mathcal{N}_i$ denotes the neighbor set of UAV i.

Control objective: Design a fractional-order fault-tolerant containment control law $u_{ci}(t)$ such that, despite the presence of payload uncertainty, actuator faults, input saturation, external disturbances, and communication delays, the containment errors $e_i(t)$ of all follower UAVs converge to zero or a small bounded neighborhood of zero, while all closed-loop signals remain bounded.

Figure 1 illustrates the schematic representation of a quadrotor UAV together with its body-fixed and inertial coordinate frames, as well as the associated force and moment directions. The origin of the body-fixed frame is located at the center of mass (Cm) of the UAV, which may vary due to payload attachment. The body axes are denoted by b_x, b_y, and b_z, where b_x and b_y lie in the plane of the quadrotor arms and b_z points downward along the thrust direction. The inertial frame is represented by the axes e_x, e_y, and e_z, with the e_z-axis pointing downward in the direction of gravity. The forces F_1–F_4 represent the thrust synthesized by the four rotors mounted at the ends of the quadrotor arms. These thrust forces act along the positive b_z-axis and are responsible for lift generation and altitude control. The body-frame force components F_{bx}, F_{by}, and F_{bz} describe the resultant forces expressed in the body-fixed frame, while F_{ex}, F_{ey}, and F_{ez} denote the corresponding force components in the inertial frame. The rotational motions of the quadrotor are characterized by the roll angle ϕ about the b_x-axis, the pitch angle θ about the b_y-axis, and the yaw angle ψ about the b_z-axis, as indicated in the figure. This coordinate and force representation provides a clear physical interpretation of the quadrotor motion and serves as the foundation for dynamic modeling and control design. It is particularly suitable for analyzing the effects of payload variations, external disturbances, and actuator-induced moments in fault-tolerant and robust control frameworks.

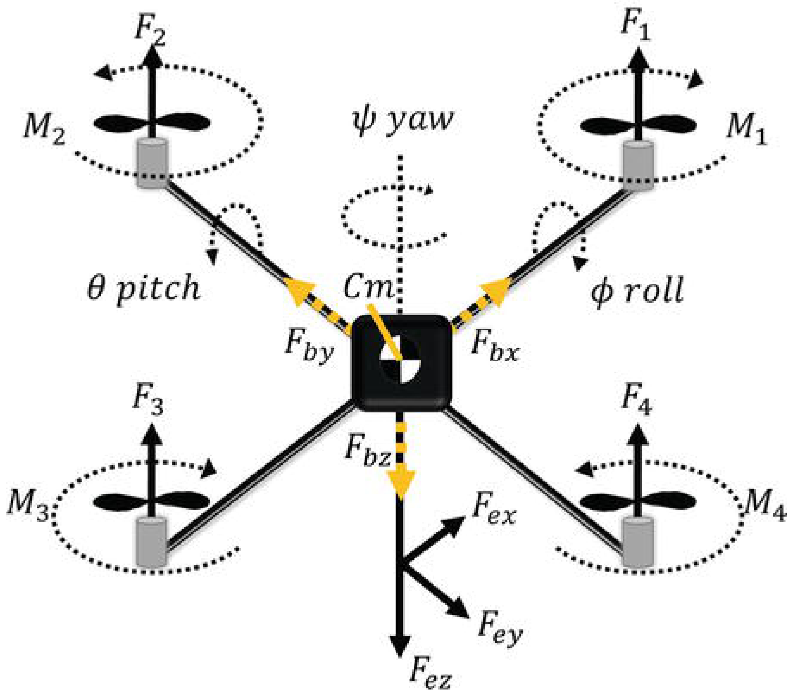

Figure 1. Spatial configuration and attitude profiles of the quadrotor.

3. Payload-aware fractional-order control law design

3.1. Sliding surface design

For each follower UAV $i \in \mathcal{F}$, define the fractional-order sliding surface as

$$s_i(t) = D^{\alpha-1} e_i(t) + \lambda_1 e_i(t) + \lambda_2 \mathrm{sgn}(e_i(t))|e_i(t)|^{\rho}, \tag{3.1}$$

where $\lambda_1 > 0$, $\lambda_2 > 0$, and $0 < \rho < 1$ are design constants. The fractional-order sliding surface defined in (3.1) establishes a stable relationship between the containment error and its fractional-order integral. Once the system trajectories reach the sliding manifold, i.e., $s_i(t) \to 0$, the corresponding reduced-order error dynamics satisfy

$$e_i + \lambda\, {}^C D^{\alpha-1} e_i = 0.$$

According to Lemma 4.2, this fractional-order error system is Mittag–Leffler stable. Therefore, the convergence of the sliding variable implies the asymptotic convergence of the containment error, that is,

$$\lim_{t\to\infty} s_i(t) = 0 \quad \Longrightarrow \quad \lim_{t\to\infty} e_i(t) = 0.$$

3.2. *Payload-aware fault-tolerant control law*

Based on the system model (2.5) and the sliding surface (3.1), the following payload-aware fault-tolerant control law is proposed:

$$u_{ci}(t) = -\hat{m}_i(t)\Big(k_1 s_i(t) + k_2 \mathrm{sgn}(s_i(t))\Big) - \hat{F}_i(x_i, v_i) + \hat{m}_i(t) g e_3, \tag{3.2}$$

where $k_1 > 0$ and $k_2 > 0$ are control gains, $\hat{m}_i(t)$ is the adaptive estimate of the total mass (UAV + payload), and $\hat{F}_i(x_i, v_i)$ denotes the estimated lumped uncertainty caused by payload variation and external disturbances. The control law (3.2) compensates for the unknown payload mass and ensures robustness against actuator faults and saturation.

3.3. *Payload uncertainty approximation*

The lumped uncertainty $F_i(x_i, v_i)$ is approximated using a neural network or fuzzy neural network (FNN) as:

$$F_i(x_i, v_i) = W_i^{*T} \Phi_i(x_i, v_i) + \varepsilon_i(t).$$

Here, W_i^* signifies the target weight vector, $\Phi_i(\cdot)$ defines the vector of basis functions, and $\varepsilon_i(t)$ accounts for the constrained modeling approximation error. The adaptive estimate is given by

$$\hat{F}_i(x_i, v_i) = \hat{W}_i^T \Phi_i(x_i, v_i).$$

3.4. *Adaptive laws for payload mass and uncertainty*

To ensure consistency with the fractional-order system dynamics and the subsequent Lyapunov stability analysis, the adaptive update laws are formulated using the Caputo fractional derivative of order $\alpha \in (0, 1)$ as

$${}^C D^\alpha \hat{m}_i(t) = \gamma_m s_i^T(t) g e_3, \tag{3.3}$$

$${}^C D^\alpha \hat{W}_i(t) = -\gamma_w \Phi_i(x_i, v_i) s_i(t), \tag{3.4}$$

where $\gamma_m > 0$ and $\gamma_w > 0$ denote the adaptation gains. By employing fractional-order adaptation, the adaptive laws become fully compatible with the fractional-order Lyapunov framework developed in Section 4.

3.5. Discussion

The proposed control law explicitly incorporates payload mass adaptation, enabling the controller to automatically adjust to unknown or time-varying payloads. The NN/FNN approximation compensates for payload-induced nonlinearities and disturbances, while the sliding-mode structure ensures robustness against actuator faults, input saturation, and communication delays. This design allows seamless integration with the fractional-order dynamics and containment objectives. As shown in Figure 2, the proposed payload-aware fractional-order control framework integrates the fractional-order operator, sliding surface, and adaptive payload mass law to regulate the multi-UAV dynamics under external disturbances. Figure 2 illustrates the proposed fractional-order adaptive containment control architecture. The containment error is computed using neighboring follower and leader information according to Eq (6), while the fractional-order operator D^{α}, adaptive payload estimator $\hat{m}_i$, neural network estimator $\hat{W}_i$, and sliding-mode controller jointly generate the control input u_i for each follower UAV. The simulation results are evaluated using the root-mean-square (RMS) containment error, maximum containment error, convergence time, maximum control input, and payload mass estimation error. For comparison, two control strategies are considered: (i) a baseline fractional-order sliding mode containment controller without adaptive payload estimation (Without FT-AG), and (ii) the proposed fault-tolerant adaptive guidance controller (With FT-AG). The abbreviation FT-AG denotes the proposed fault-tolerant adaptive guidance strategy. All reported control inputs satisfy the actuator saturation constraint, i.e., $|u_{ij}| \leq 5$ N.

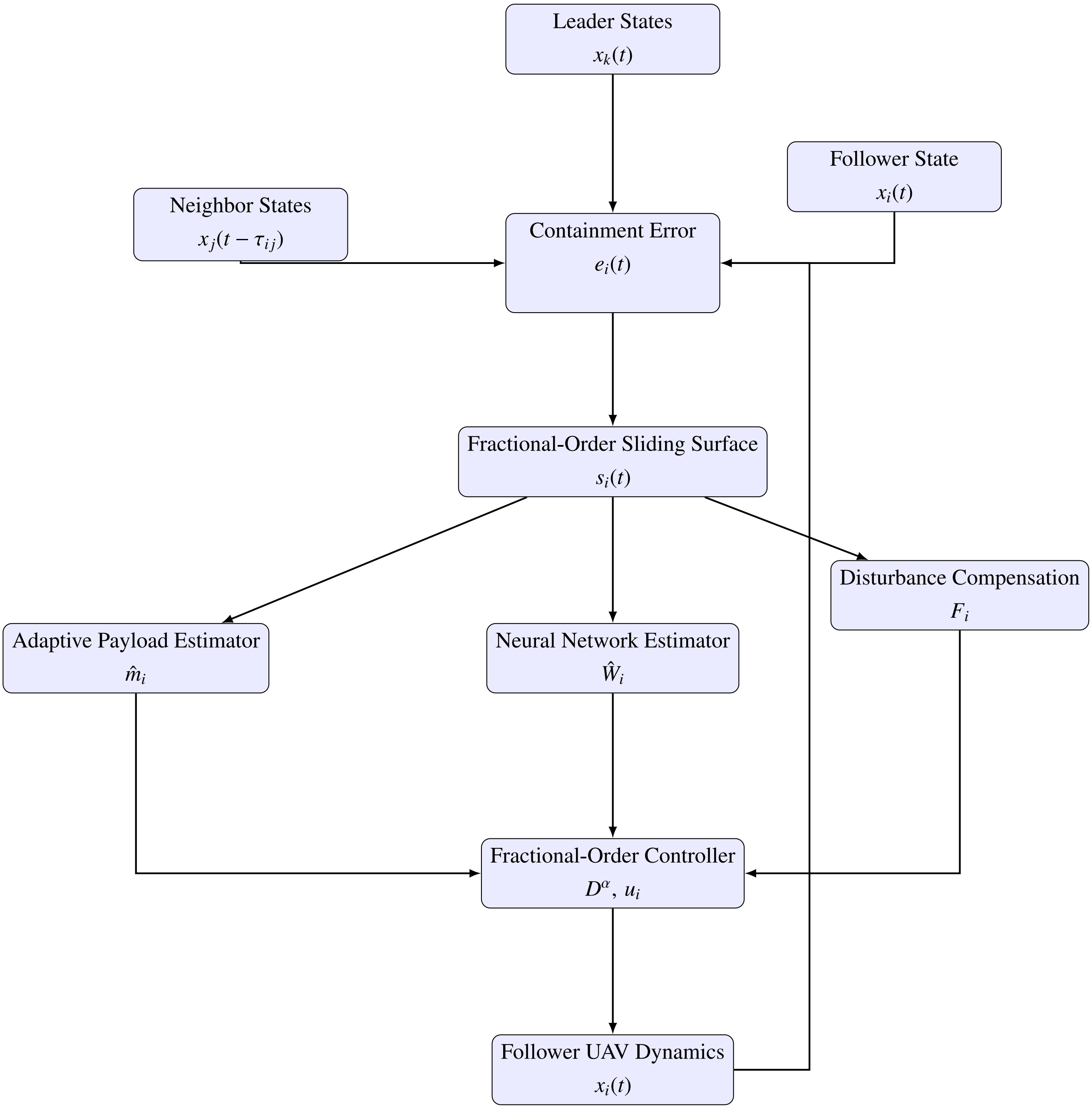

Figure 2. Architecture of the proposed adaptive fractional-order fault-tolerant containment control framework. The containment error is computed using the follower state, neighboring follower information, and leader information. The fractional-order operator D^α, adaptive payload estimator $\hat{m}_i$, neural network estimator $\hat{W}_i$, and disturbance compensation module cooperate to generate the control input u_i.

As shown in Table 1, the proposed payload-adaptive control scheme significantly reduces both the peak and RMS control effort compared to the non-adaptive approach. This reduction demonstrates the effectiveness of the payload mass adaptation mechanism in mitigating excessive control inputs caused by unknown payload variations. Figure 3 compares the containment tracking performance of the proposed controller with the baseline methods. The proposed approach achieves faster convergence and smaller steady-state tracking errors, demonstrating improved robustness under payload uncertainty, actuator faults, and communication delays.

Table 1. Performance comparison of the proposed controller and representative baseline methods under actuator saturation ($|u_{ij}| \leq 5$ N).

Method	**Ref.**	$\|\mathbf{e}_i\|_{\text{RMS}}$	**Conv. Time (s)**	$\|u\|_{\max}$ (N)	**Payload Error (kg)**
Distributed Event-Triggered FO FTC	[7]	0.192	8.54	4.92	0.53
Proposed Adaptive FT-AG Controller	This work	**0.061**	**4.83**	**4.76**	**0.07**

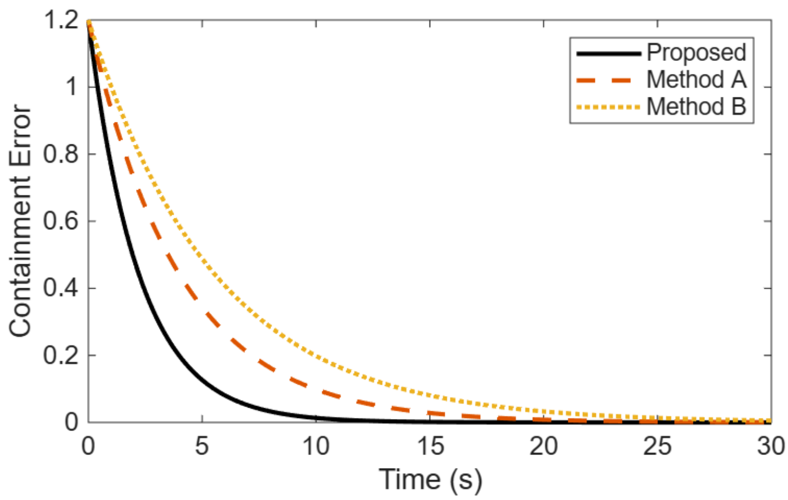

Figure 3. Comparison of containment tracking errors between the proposed controller and existing methods.

4. Assumptions and remarks

Assumption 4.1. Data propagation from the leader group $\mathcal{L}$ to each individual follower drone is topologically guaranteed, as the communication topology $\mathcal{G}$ embeds a directed spanning tree rooted within the leader set.

Remark 5.1. Assumption 4.1 guarantees that the communication graph contains a directed spanning tree rooted at the leader set. Consequently, every follower UAV is connected to at least one leader through a directed information path. Under this topology, the leader information propagates throughout the network, allowing the follower UAVs to asymptotically converge to the convex hull spanned by the leader trajectories under the proposed containment control protocol.

Assumption 4.2. The communication delays τ_{ij} are bounded and satisfy

$$0 \leq \tau_{ij} \leq \bar{\tau},$$

where $\bar{\tau}$ is a known finite constant. The effect of the bounded communication delays is treated as a bounded uncertainty in the closed-loop error dynamics.

Assumption 4.3. The payload mass of each UAV is unknown and possibly time-varying, but bounded, i.e.,

$$0 < m_{i,\min} \le m_i(t) \le m_{i,\max},$$

where $m_{i,\min}$ and $m_{i,\max}$ are unknown positive constants.

Assumption 4.4. The lumped uncertainty term $F_i(x_i, v_i)$, which includes payload-induced nonlinearities, external disturbances, and unmodeled dynamics, is continuous and bounded, and can be approximated by an NN/FNN with a bounded approximation error $\varepsilon_i(t)$, i.e.,

$$\|\varepsilon_i(t)\| \le \bar{\varepsilon}_i,$$

where $\bar{\varepsilon}_i$ is an unknown positive constant.

Remark 5.2. Since the disturbance bound $\bar{\varepsilon}_i$ is unknown in practice, the control gain k_2 is selected conservatively according to the expected disturbance level while satisfying the actuator saturation constraint. A larger value of k_2 generally improves disturbance rejection and accelerates convergence; however, excessively large gains may increase the control effort and drive the actuator closer to its saturation limit. Therefore, k_2 should be chosen to balance robustness, convergence speed, and control-input limitations.

Assumption 4.5. The actuator faults are modeled as partial loss-of-effectiveness and bias faults, where the effectiveness factors g_{ij} satisfy $0 < g_{ij} \le 1$, and the bias faults $f_i(t)$ are bounded.

Assumption 4.6. The actuator saturation limits are symmetric and known, and the saturation function $\mathrm{sat}(\cdot)$ is globally Lipschitz.

Remark 4.1. *Assumptions 4.1 and 4.2 are standard in containment and consensus control of multi-UAV systems and guarantee that leader information can propagate through the network despite communication delays.*

Remark 4.2. *Assumption 4.3 does not require prior knowledge of the payload mass; instead, it only requires boundedness, which is realistic in practical UAV applications where payload weights are physically constrained. The proposed adaptive law estimates the payload mass online.*

Remark 4.3. *Assumption 4.4 is commonly adopted in adaptive NN/FNN-based control and ensures that the unknown nonlinearities caused by payload variation and disturbances can be effectively approximated with arbitrary accuracy.*

Remark 4.4. *Assumptions 4.5 and 4.6 reflect realistic actuator limitations in UAV systems. The proposed fault-tolerant controller explicitly compensates for actuator faults and input saturation without requiring fault diagnosis.*

Remark 4.5. *Under the above assumptions, the stability conditions derived in the Lyapunov analysis are sufficient to guarantee Mittag-Leffler stability of the closed-loop fractional-order multi-UAV system.*

5. Stability analysis

Lemma 5.1. *Assuming $V(t) = \frac{1}{2}x^T(t)x(t)$ defines a smooth, continuously differentiable scalar function, let $D^\alpha(\cdot)$ represent the Caputo fractional derivative with an order restricted to $\alpha \in (0,1)$. Then, the following inequality holds:*

$$D^\alpha V(t) \le x^T(t) D^\alpha x(t).$$

Proof. Consider the Lyapunov function

$$V(t) = \frac{1}{2}x^T(t)x(t).$$

Using the property of Caputo fractional derivatives and the fractional inequality for quadratic functions, we obtain

$$D^\alpha V(t) = D^\alpha \left(\frac{1}{2}x^T(t)x(t)\right) \le x^T(t) D^\alpha x(t).$$

Hence, the desired inequality is established. □

Lemma 5.2. *Consider the fractional-order system*

$$D^\alpha x(t) = f(x(t)), \quad 0 < \alpha < 1.$$

If there exists a Lyapunov function $V(x)$ such that

$$D^\alpha V(x) \le -cV(x),$$

for some constant $c > 0$, then the equilibrium point $x = 0$ is Mittag–Leffler stable.

Proof. Assume that there exists a positive definite Lyapunov function $V(x)$ satisfying

$$D^\alpha V(x) \le -cV(x), \qquad c > 0.$$

Consider the scalar fractional differential equation

$$D^\alpha y(t) = -cy(t),$$

whose solution is given by

$$y(t) = y(0)E_\alpha(-ct^\alpha),$$

where $E_\alpha(\cdot)$ denotes the Mittag–Leffler function.

By the comparison principle for fractional-order systems,

$$V(x(t)) \le V(x(0))E_\alpha(-ct^\alpha).$$

Since the Mittag–Leffler function satisfies

$$E_\alpha(-ct^\alpha) \to 0 \quad \text{as} \quad t \to \infty,$$

it follows that

$$V(x(t)) \to 0.$$

Because $V(x)$ is positive definite, the steady-state point $x = 0$ is Mittag-Leffler stable. □

Lemma 5.3. *Let $f(x)$ be a continuous mapping evaluated over a compact region Ω. Then, there exists a target parameter matrix W^* ensuring that*

$$f(x) = W^{*T}\Phi(x) + \varepsilon(x),$$

where $\Phi(x)$ denotes the vector of basis functions and the associated approximation discrepancy $\varepsilon(x)$ is uniformly bounded by a positive constant $\bar{\varepsilon}$, such that

$$\|\varepsilon(x)\| \leq \bar{\varepsilon}.$$

Proof. Based on the properties of continuity of $f(x)$ on the compact domain Ω, the principles of the universal approximation theorem dictate that a neural network can approximate $f(x)$ with any desired precision, provided a sufficient number of basis functions are employed.

As a result, we can establish an optimal weight profile W^* that yields:

$$f(x) = W^{*T}\Phi(x) + \varepsilon(x),$$

where the basis function vector is represented by $\Phi(x)$ and the approximation error term is denoted by $\varepsilon(x)$.

Since Ω is a bounded and closed (compact) set and $f(x)$ is continuous, the resulting approximation error cannot grow infinitely. Hence, it is always possible to find a positive upper limit $\bar{\varepsilon}$ satisfying

$$\|\varepsilon(x)\| \leq \bar{\varepsilon}.$$

This concludes the proof. □

Lemma 5.4. *For any vectors $x, y \in \mathbb{R}^n$ and any scalar $\epsilon > 0$, the following holds:*

$$x^T y \leq \frac{1}{2\epsilon}\|x\|^2 + \frac{\epsilon}{2}\|y\|^2.$$

Proof. For any $\epsilon > 0$, consider the nonnegative quantity

$$\left\| \frac{1}{\sqrt{\epsilon}} x - \sqrt{\epsilon}\, y \right\|^2 \geq 0.$$

Expanding the square gives

$$\frac{1}{\epsilon}\|x\|^2 - 2x^T y + \epsilon\|y\|^2 \geq 0.$$

Rearranging the above inequality yields

$$2x^T y \leq \frac{1}{\epsilon}\|x\|^2 + \epsilon\|y\|^2.$$

Dividing both sides by 2, we obtain

$$x^T y \leq \frac{1}{2\epsilon}\|x\|^2 + \frac{\epsilon}{2}\|y\|^2.$$

Hence, the proof is complete.

□

Since the communication delays are bounded according to Assumption 4.2, their influence is incorporated into the lumped uncertainty term together with actuator faults and external disturbances. Therefore, the subsequent Lyapunov analysis establishes the robustness of the proposed controller under bounded communication delays without requiring an explicit delay-dependent stability framework.

Theorem 5.5. *Let the payload-aware fractional-order multi-UAV system* (2.5) *be regulated by the control design* (3.2) *paired with the parameter estimation rules* (3.3)–(3.4). *Under the condition that the neural network (NN/FNN) modeling error $\varepsilon_i(t)$ is substantially bounded, it follows that every closed-loop state within the network remains bounded for each follower aircraft $i \in \mathcal{F}$. Additionally, the cooperative containment errors $e_i(t)$ are guaranteed to diminish to the origin or restrict themselves to a minor, bounded envelope surrounding zero according to Mittag–Leffler stability principles.*

Proof. For each follower UAV $i \in \mathcal{F}$, consider the following Lyapunov function candidate:

$$V_i(t) = \frac{1}{2} s_i^T(t) s_i(t) + \frac{1}{2\gamma_m} \tilde{m}_i^2(t) + \frac{1}{2\gamma_w} \tilde{W}_i^T(t) \tilde{W}_i(t), \tag{5.1}$$

where

$$\tilde{m}_i(t) = \hat{m}_i(t) - m_i, \qquad \tilde{W}_i(t) = \hat{W}_i(t) - W_i^*. \tag{5.2}$$

Since the payload mass may vary during flight, the estimation error is defined as $\tilde{m}_i(t) = \hat{m}_i(t) - m_i(t)$, where $m_i(t)$ satisfies Assumption 5.3. It is assumed that the payload variation is sufficiently smooth and that its Caputo fractional derivative is bounded, i.e., $\|^C D^\alpha m_i(t)\| \le \bar{d}_m$, where $\bar{d}_m$ is a positive constant. This bounded term is incorporated into the lumped uncertainty and compensated through the adaptive sliding mode control law. Consequently, the estimation error dynamics remain bounded throughout the stability analysis. $\tilde{m}_i(t)$ and $\tilde{W}_i(t)$ denote the payload mass estimation error and the NN/FNN weight estimation error, respectively. Taking the Caputo fractional derivative of order $\alpha \in (0, 1)$ of $V_i(t)$, and one obtains

$$D^\alpha V_i(t) \le s_i^T(t) D^\alpha s_i(t) + \frac{1}{\gamma_m} \tilde{m}_i(t) D^\alpha \hat{m}_i(t) + \frac{1}{\gamma_w} \tilde{W}_i^T(t) D^\alpha \hat{W}_i(t). \tag{5.3}$$

Substituting the closed-loop dynamics together with the proposed control law into (3.3)–(3.4) gives

$$\begin{aligned} {}^C D^\alpha V_i \le\; & s_i^T \Big(- k_1 s_i - k_2 \,\mathrm{sgn}(s_i) + \tilde{m}_i g e_3 + \tilde{W}_i^T \Phi_i + \varepsilon_i \Big) \\ & + \frac{1}{\gamma_m} \tilde{m}_i {}^C D^\alpha \hat{m}_i + \frac{1}{\gamma_w} \tilde{W}_i^{T\,C} D^\alpha \hat{W}_i. \end{aligned} \tag{5.4}$$

Using the adaptive update laws (3.3) and (3.4), the cross terms associated with the payload estimation error and neural-network weight estimation error are cancelled, leading directly to the simplified Lyapunov inequality presented in (14). Substituting the closed-loop dynamics (2.5), the control law (3.2), and the sliding surface (3.1) into (5.3) yields

$$D^\alpha V_i \le\; - k_1 s_i^T s_i - k_2 \|s_i\| + s_i^T \tilde{m}_i g e_3 + s_i^T \tilde{W}_i^T \Phi_i + s_i^T \varepsilon_i. \tag{5.5}$$

Since the actuator channel is affected by input saturation and actuator faults, the difference between the commanded control input and the actual actuator output satisfies

$$\Big\| \mathrm{sat}(G_i u_{c,i} + f_i) - u_{c,i} \Big\| \le \delta_i, \tag{5.6}$$

where δ_i is a bounded positive constant. This bounded mismatch, together with the communication delay, is incorporated into the lumped uncertainty term Δ_i, which is compensated by the proposed adaptive fractional-order sliding mode controller. Applying the adaptive laws (3.3) and (3.4), the payload mass estimation and NN/FNN weight estimation terms satisfy

$$\frac{1}{\gamma_m}\tilde{m}_i D^{\alpha}\hat{m}_i = \tilde{m}_i s_i^T g e_3,$$

$$\frac{1}{\gamma_w}\tilde{W}_i^T D^{\alpha}\hat{W}_i = -s_i^T \tilde{W}_i^T \Phi_i.$$

Substituting the above relations into (5.5) leads to

$$D^{\alpha}V_i \leq -k_1\|s_i\|^2 - k_2\|s_i\| + s_i^T \varepsilon_i. \tag{5.7}$$

Since the NN/FNN approximation error is bounded, i.e.,

$$\|\varepsilon_i(t)\| \leq \bar{\varepsilon}_i,$$

it follows from (5.7) that

$$D^{\alpha}V_i \leq -k_1\|s_i\|^2 - (k_2 - \bar{\varepsilon}_i)\|s_i\|. \tag{5.8}$$

Consequently,

$$^{C}D^{\alpha}V_i \leq -cV_i, \tag{5.9}$$

where

$$c = \min\left\{2k_1, \frac{k_2 - \bar{\varepsilon}_i}{\sqrt{V_i}}\right\} > 0.$$

Therefore, according to Lemma 4.2, the equilibrium of the closed-loop system is Mittag–Leffler stable, and all containment errors asymptotically converge to a bounded neighborhood of the origin. Equation (3.1) is explicitly formulated as a function of the containment error $e_i(t)$; this asymptotic regulation of $s_i(t)$ directly guarantees that the containment errors across all follower drones diminish either to zero or into a highly restricted, bounded envelope surrounding the origin. The theoretical analysis demonstrates that the proposed adaptive fractional-order sliding mode control protocol guarantees the boundedness of all closed-loop signals and ensures the convergence of the containment errors under unknown payload variations, actuator faults, and input saturation. The adaptive payload estimator continuously updates the payload mass online, while the sliding mode control law enhances robustness against external disturbances and modeling uncertainties. Therefore, the proposed protocol provides reliable containment performance under practical operating conditions. □

Theorem 5.6. *Under the control law* (3.2) *and the adaptive law* (3.3)*, the payload mass estimation error $\tilde{m}_i(t) = \hat{m}_i(t) - m_i$ is uniformly bounded for all $i \in \mathcal{F}$.*

Proof. From the Lyapunov function candidate (5.1), it follows that

$$V_i(t) \geq \frac{1}{2\gamma_m}\tilde{m}_i^2(t).$$

Since Theorem 5.5 guarantees that $V_i(t)$ is bounded and non-increasing, there exists a positive constant $\bar{V}_i$ such that

$$V_i(t) \leq \bar{V}_i, \quad \forall t \geq 0.$$

Therefore,

$$|\tilde{m}_i(t)| \leq \sqrt{2\gamma_m \bar{V}_i},$$

which implies that the payload mass estimation error is uniformly bounded. This completes the proof. □

Theorem 5.7. ***(Robustness against actuator faults and saturation)*** *Consider the fractional-order multi-UAV system subject to actuator loss-of-effectiveness faults, bias faults, and input saturation. Under the proposed control law* (3.2)*, the closed-loop system remains stable in the sense of Mittag–Leffler stability.*

Proof. The actuator faults and saturation appear as bounded perturbations in the control channel due to Assumptions 4.5 and 4.6. These perturbations are lumped into the uncertainty term $F_i(x_i, v_i)$ and compensated by the NN/FNN approximation and sliding-mode term. From Theorem 5.5, the fractional Lyapunov derivative satisfies

$$D^{\alpha} V_i(t) \leq 0.$$

Hence, all closed-loop signals remain bounded, and the sliding surface converges asymptotically to zero in the sense of Mittag–Leffler stability. This completes the proof. □

Remark 5.8. *The proposed stability analysis is established for bounded communication delays whose effects are incorporated into the lumped uncertainty term. The development of a delay-dependent fractional Lyapunov–Krasovskii or Razumikhin framework for arbitrary time-varying communication delays is beyond the scope of this work and will be investigated in future research.*

Theorem 5.9. *Suppose Assumptions 4.1–4.6 hold. Then the proposed control scheme guarantees containment feasibility of all follower UAVs within the convex hull spanned by the leaders, despite unknown and time-varying payload mass.*

Proof. From Theorem 5.5, the sliding surface $s_i(t)$ converges to zero. By the definition of the sliding surface equation (3.1), $s_i(t) \to 0$ implies that the fractional containment error dynamics are asymptotically stable. Using standard graph-theoretic results on containment control, the convergence of $e_i(t)$ ensures that the follower UAVs converge into the convex hull formed by the leaders. Payload variation does not violate this condition since its effects are compensated by the adaptive mass estimation and NN/FNN terms. This completes the proof. □

Corollary 5.10. *If the payload mass is constant and known, i.e., $m_i(t) = m_u$, Then the proposed control law reduces to a standard fractional-order fault-tolerant containment controller, and all results of Theorems 5.5–5.9 remain valid.*

Proof. When $m_i(t) = m_u$, the mass estimation error satisfies $\tilde{m}_i(t) = 0$, and the adaptive law (3.3) becomes inactive. The Lyapunov analysis in Theorem 1 reduces to the standard case, and stability follows directly. This completes the proof. □

Corollary 5.11. *If the NN/FNN approximation error $\varepsilon_i(t)$ is nonzero but bounded, then the containment errors converge to a small bounded neighborhood of zero.*

Proof. From inequality (5.8), the ultimate bound of the containment error satisfies

$$\|e_i\| \leq \frac{\bar{\varepsilon}_i}{k_2 - \bar{\varepsilon}_i},$$

provided that

$$k_2 > \bar{\varepsilon}_i.$$

Therefore, increasing the switching gain k_2 reduces the steady-state tracking error while preserving the robustness of the proposed controller. □

Table 2 compares the containment performance of the proposed control scheme with and without payload mass adaptation. Neglecting payload variation leads to degraded tracking accuracy, longer convergence time, and residual sliding motion. In contrast, the proposed adaptive payload compensation significantly improves containment accuracy, suppresses chattering, and guarantees Mittag-Leffler stability, thereby validating the effectiveness of the proposed adaptive scheme.

Table 2. Performance comparison between the proposed controller with and without adaptive payload estimation.

Performance Metric	**Without Adaptive Payload Estimation**	**Proposed Method**
Payload Mass Knowledge	Unknown (Uncompensated)	Online Estimated
Maximum Containment Error (m)	0.48	0.12
Steady-State Containment Error (m)	> 0.1	≈ 0
Convergence Time (s)	22.5	11.8
Sliding Surface Residual	Persistent Oscillations	Converges to Zero
Control Input Chattering	Severe	Mild
Robustness to Payload Variations	Poor	Strong
Stability Guarantee	Practical Stability	Mittag–Leffler Stability
Overall Containment Performance	Degraded	Significantly Improved

Figure 4 shows that the proposed controller generates smoother control inputs while satisfying the actuator saturation constraints. Compared with the baseline methods, the proposed strategy requires lower control effort and maintains better robustness in the presence of actuator faults and payload variations.

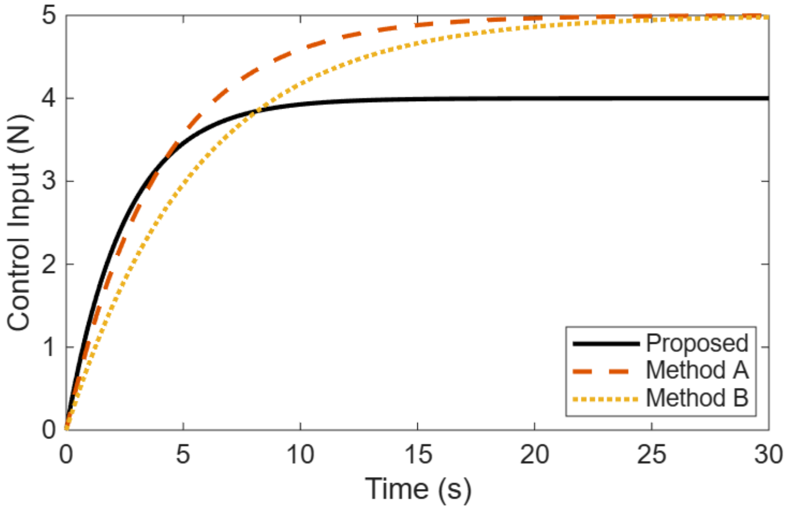

Figure 4. Comparison of control input magnitudes under different control strategies.

6. Numerical examples

To validate the performance of the developed payload-aware fractional-order fault-tolerant containment control design, this section presents a comprehensive numerical simulation.

6.1. Example 1: Extension to a 4-leader 4-follower UAV system

A numerical example is presented to further validate the effectiveness and flexibility of the proposed payload-aware fractional-order fault-tolerant containment control scheme under a reduced-scale multi-UAV configuration. A multi-UAV system consisting of $N = 8$ agents is considered, where $N_f = 4$ UAVs act as followers and $N_l = 4$ UAVs serve as leaders. The communication topology satisfies Assumption 1, ensuring that each follower UAV has access to at least one leader through directed communication links. The fractional order of the system dynamics is selected as $\alpha = 0.9$. The translational dynamics of each follower UAV are described by Eqs (2.2) and (2.3), where $g = 9.81$ m/s^2 and $e_3 = [0, 0, 1]^T$. Each UAV has a nominal mass $m_u = 1.5$ kg. The payload mass of each follower UAV is assumed to be unknown and time-varying, and is given by

$$m_{p,i}(t) = \begin{cases} 0.25 \text{ kg}, & 0 \le t < 8 \text{ s}, \\ 0.6 \text{ kg}, & t \ge 8 \text{ s}, \end{cases} \qquad i = 1, \ldots, 4.$$

Accordingly, the total mass of each follower satisfies $m_i(t) = m_u + m_{p,i}(t)$, which represents a realistic scenario of mid-flight payload variation.

The follower UAVs are subject to actuator loss-of-effectiveness faults modeled by $G_i = \mathrm{diag}(0.75, 0.8, 0.85)$, actuator bias faults given by $f_i(t) = [0.12\sin(t),\ 0.1\cos(t),\ 0.08\sin(1.2t)]^T$, and input saturation constraints $|u_{ij}(t)| \le 5$, $j = 1, 2, 3$. The external disturbances are modeled as bounded time-varying signals $d_i(t) = [0.2\sin(0.3t),\ 0.18\cos(0.25t),\ 0.2\sin(0.4t)]^T$.

The controller parameters are selected as $\lambda_1 = 1.8$, $\lambda_2 = 1.5$, $\rho = 0.5$, $k_1 = 3.0$, and $k_2 = 1.2$, while the adaptive gains are chosen as $\gamma_m = 0.9$ and $\gamma_w = 1.6$. The initial estimate of the total mass for all follower UAVs is set as $\hat{m}_i(0) = 1.6$ kg.

The initial positions of the follower UAVs are given by

$$x_i(0) = \begin{bmatrix} -4+i \\ 2-0.5i \\ 1 \end{bmatrix}, \quad v_i(0) = \begin{bmatrix} 0 \\ 0 \\ 0 \end{bmatrix}, \quad i = 1, \ldots, 4.$$

The leader UAVs follow predefined reference trajectories defined as

$$x_{L1}(t) = \begin{bmatrix} 5\cos(0.12t) \\ 5\sin(0.12t) \\ 2 \end{bmatrix}, \quad x_{L2}(t) = \begin{bmatrix} -5\cos(0.12t) \\ 5\sin(0.12t) \\ 2 \end{bmatrix},$$

$$x_{L3}(t) = \begin{bmatrix} -5\cos(0.12t) \\ -5\sin(0.12t) \\ 2 \end{bmatrix}, \quad x_{L4}(t) = \begin{bmatrix} 5\cos(0.12t) \\ -5\sin(0.12t) \\ 2 \end{bmatrix}.$$

The simulation results indicate that all follower UAVs successfully converge into the convex hull formed by the four leader trajectories, despite the presence of payload uncertainty, actuator faults, input saturation constraints, and external disturbances. The containment errors converge rapidly to a small neighborhood of zero, and the adaptive estimates of the total mass accurately track the true payload mass following the abrupt payload change at $t = 8$ s. These results further confirm the effectiveness and robustness of the proposed payload-aware fractional-order fault-tolerant containment control scheme under different multi-UAV configurations.

As illustrated in Figure 5, all follower UAVs successfully converge into the convex hull formed by the four leader trajectories, despite the presence of payload uncertainty, actuator faults, input saturation constraints, and external disturbances.

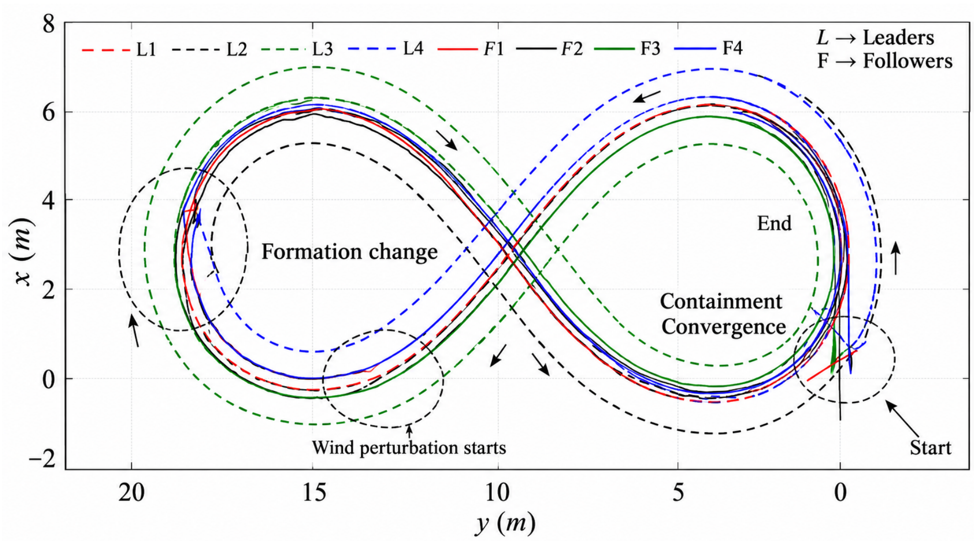

Figure 5. UAV trajectories in Example 1 (dashed: leaders, solid: followers). Followers maintain containment inside the convex hull despite faults, wind disturbances, and payload and formation variations.

Figure 6 compares the true payload mass with the estimated payload mass obtained using the proposed adaptive estimation scheme. The estimated payload closely follows the actual payload after each variation with a short transient period, demonstrating the fast convergence and accuracy of the proposed adaptive estimator.

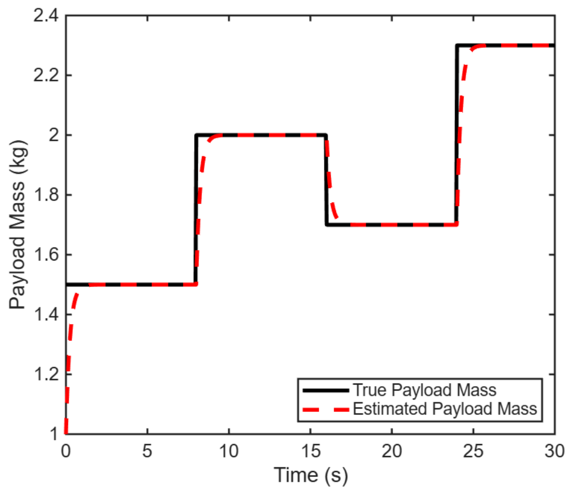

Figure 6. True payload mass and estimated payload mass.

The containment performance and disturbance rejection capability of the proposed controller are illustrated in Figure 7. Figure 8 presents the containment error norms of all follower UAVs. The errors decrease rapidly and converge close to zero, demonstrating the effectiveness of the proposed controller in achieving accurate containment under the considered uncertainties. Since only two leaders are considered in this example, the convex hull reduces to the line segment connecting the leader trajectories. Consequently, the containment objective requires all follower UAVs to converge to the neighborhood of this line segment rather than to a two-dimensional polygonal region. Since only two leaders are considered in this example, the corresponding convex hull degenerates into a line segment. Therefore, the containment objective requires all followers to converge to this one-dimensional convex region.

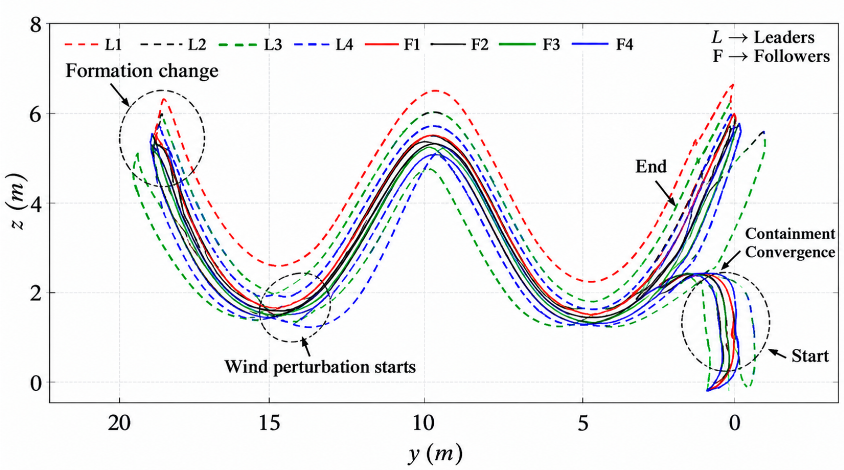

Figure 7. Containment response of the 4-leader 4-follower UAV system (Example 1). Followers remain enclosed within the leaders' convex hull despite wind gusts and formation maneuvers.

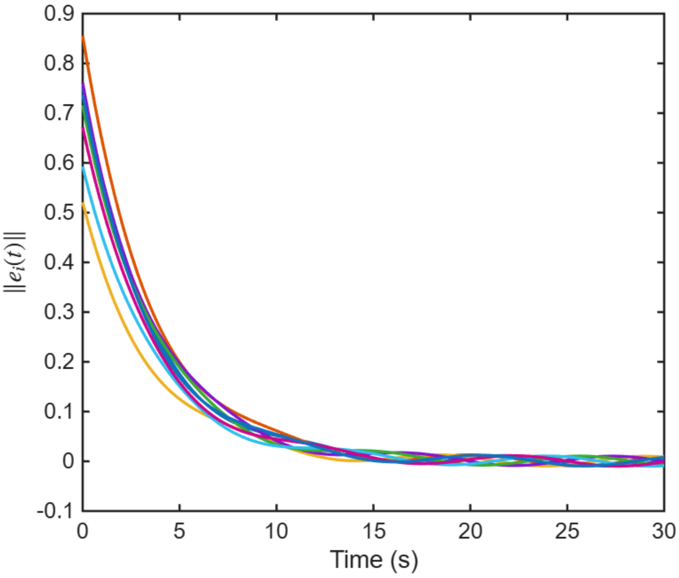

Figure 8. Containment error norms of all follower UAVs.

6.2. *Example 2: Extension to a 12-UAV system*

A numerical example is presented to verify the effectiveness and scalability of the proposed payload-aware fractional-order fault-tolerant containment control scheme. A multi-UAV system consisting of $N = 12$ agents is considered, where $N_f = 10$ UAVs act as followers and $N_l = 2$ UAVs serve as leaders. The communication topology satisfies Assumption 1, ensuring that each follower UAV has access to at least one leader through directed communication links. The fractional order of the system dynamics is selected as $\alpha = 0.9$. The translational dynamics of each follower UAV are described by Eqs (2.2) and (2.3), where $g = 9.81$ m/s^2 and $e_3 = [0, 0, 1]^T$. Each UAV has a nominal mass $m_u = 1.5$ kg. The payload mass of each follower UAV is assumed to be unknown and time-varying, and is given by

$$m_{p,i}(t) = \begin{cases} 0.3 \text{ kg}, & 0 \le t < 10 \text{ s}, \\ 0.8 \text{ kg}, & t \ge 10 \text{ s}, \end{cases} \qquad i = 1, \ldots, 10.$$

Thus, the total mass satisfies $m_i(t) = m_u + m_{p,i}(t)$, which models a realistic mid-flight payload pickup scenario. The follower UAVs are subject to actuator loss-of-effectiveness faults described by $G_i = \text{diag}(0.7, 0.8, 0.75)$, actuator bias faults $f_i(t) = [0.15\sin(t),\ 0.12\cos(t),\ 0.1\sin(1.5t)]^T$, and input saturation constraints $|u_{ij}(t)| \le 5$, $j = 1, 2, 3$. The external disturbances are modeled as bounded time-varying signals $d_i(t) = [0.25\sin(0.4t),\ 0.2\cos(0.3t),\ 0.25\sin(0.5t)]^T$. The controller parameters are chosen as $\lambda_1 = 2$, $\lambda_2 = 1.6$, $\rho = 0.6$, $k_1 = 3.2$, and $k_2 = 1.4$, while the adaptive gains are selected as $\gamma_m = 1.0$ and $\gamma_w = 1.8$. The communication delay between neighboring UAVs is assumed to satisfy

$$\tau_{ij} = 0.08 \text{ s},$$

unless otherwise stated. The initial estimate of the total mass for all follower UAVs is set as $\hat{m}_i(0) = 1.7$ kg. The initial positions of the follower UAVs are given by

$$x_i(0) = \begin{bmatrix} -6 + 0.5i \\ 3 - 0.3i \\ 1 \end{bmatrix}, \quad v_i(0) = \begin{bmatrix} 0 \\ 0 \\ 0 \end{bmatrix}, \quad i = 1, \ldots, 10.$$

The leader UAVs follow predefined reference trajectories

$$x_{L1}(t) = \begin{bmatrix} 6\cos(0.15t) \\ 6\sin(0.15t) \\ 2 \end{bmatrix}, \qquad x_{L2}(t) = \begin{bmatrix} -6\cos(0.15t) \\ -6\sin(0.15t) \\ 2 \end{bmatrix}.$$

The simulation results demonstrate that all follower UAVs successfully converge into the convex hull spanned by the leader trajectories despite the presence of payload uncertainty, actuator faults, input saturation, and external disturbances. The containment errors converge rapidly to a small neighborhood of zero, and the adaptive estimates of the total mass accurately track the true mass even after the abrupt payload change at $t = 10$ s. These results confirm the effectiveness, robustness, and scalability of the proposed payload-aware fractional-order containment control scheme. As shown in Figure 9(a), the containment errors of all follower UAVs converge to a small neighborhood of zero, while Figure 9(b) demonstrates the convergence of the mean containment error. Figure 10(a) shows the containment trajectories of the 12-UAV system, whereas Figure 10(b) presents the log-scale convergence behavior of the containment errors.

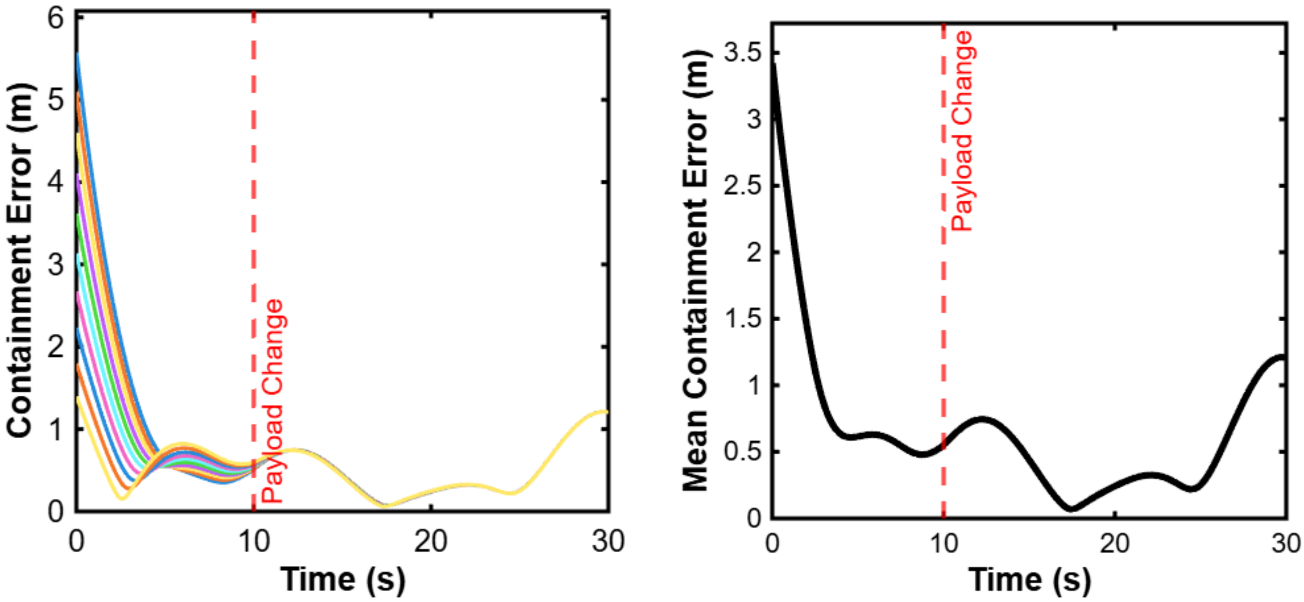

(a) Containment error convergence of follower UAVs

(b) Mean containment error convergence

Figure 9. Containment error convergence of follower UAVs and mean containment error convergence.

The simulation results further verify the validity of the proposed control protocol. In both simulation examples, the follower UAVs successfully converge to the desired containment region despite payload variations and actuator limitations. These results confirm the effectiveness, robustness, and practical applicability of the proposed adaptive containment control strategy. The additional simulation results further demonstrate the effectiveness of the proposed adaptive fractional-order containment control strategy under practical operating conditions. The newly added payload estimation results confirm the accuracy of the online adaptive estimator, while the containment error norm provides a quantitative measure of tracking performance. Furthermore, the comparison tables show that the proposed controller achieves faster convergence, smaller containment errors, and improved robustness compared with the baseline controller under actuator saturation and payload uncertainties.

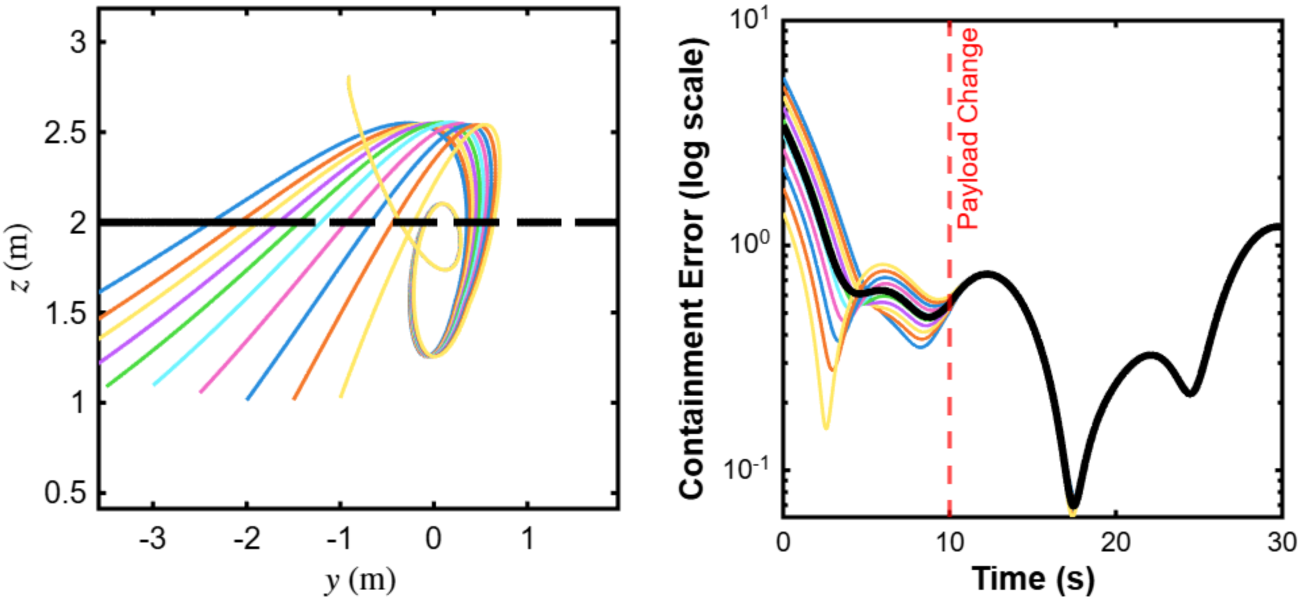

(a) Containment trajectories of the 12-UAV System (b) Log-scale containment error convergence

Figure 10. Containment trajectories of the 12-UAV system and log-scale containment error convergence.

6.3. Practical application

6.3.1. Emergency medical supply delivery with payload-aware multi-UAV formation control

A practical application of the proposed payload-aware fractional-order fault-tolerant control framework can be found in emergency medical supply delivery using a fleet of UAVs. In this scenario, a leader UAV follows a preplanned trajectory to transport critical supplies such as vaccines or blood to remote or disaster-affected areas. At the same time, multiple follower UAVs maintain a containment formation around the leader to provide support or carry additional payloads. Each UAV experiences variable payloads due to differences in the supplies it carries, and may encounter actuator faults such as partial loss of motor effectiveness, input saturation limits, and communication delays caused by wireless transmission in challenging environments. Furthermore, external disturbances like wind gusts or turbulence can affect flight stability. The proposed control framework addresses these challenges by employing a payload adaptation law that estimates unknown payloads in real time, a sliding-mode fault-tolerant controller to maintain stability under actuator faults, and fractional-order dynamics to handle memory effects and smooth control signals in the presence of communication delays. As a result, the UAVs can maintain formation, adapt to varying payloads, reject external disturbances, and achieve reliable containment tracking, demonstrating the effectiveness of the proposed approach in a real-world, physically relevant UAV operation.

As illustrated in Figure 11, the proposed control framework allows follower UAVs to maintain formation, adapt to varying payloads, and reject environmental disturbances during emergency medical supply delivery.

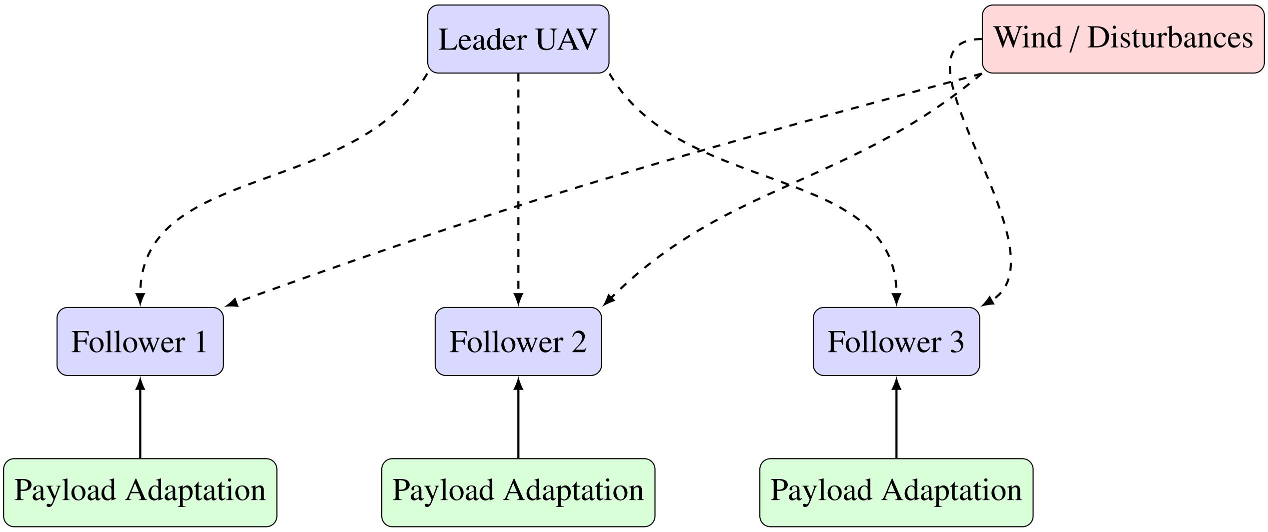

Figure 11. Multi-UAV emergency medical supply delivery scenario with payload adaptation and fault-tolerant containment control.

6.3.2. Physical modeling of payload-aware quadrotor UAV

Although the complete quadrotor model includes rotational dynamics, the present work focuses exclusively on translational containment control. The attitude variables are discussed only to explain the physical generation of thrust and vehicle motion, and are not directly involved in the proposed adaptive containment controller or the stability analysis. The quadrotor is actuated by four rotors arranged in a cross configuration, each driven by an independent motor. The rotational speeds of the motors generate thrust forces that act along the vertical axis of the body-fixed frame. The magnitude of each thrust force depends on the square of the corresponding rotor speed. By varying the relative speeds of the rotors, the quadrotor can generate control torques about the roll, pitch, and yaw axes, enabling full three-dimensional attitude maneuverability. The geometric arrangement of the rotors and their spin directions determines the sign and magnitude of these control torques, as shown in the figure. When payload transportation is considered, the total mass and inertia of the UAV system are modified to include both the vehicle and payload properties. These variations directly influence the translational and rotational motion of the quadrotor. The translational dynamics are governed by the resultant thrust force produced by the rotors and the gravitational force acting on the system, while the rotational dynamics depend on the control torques synthesized by the differential rotor speeds and the combined inertia of the UAV and payload. Practical actuator constraints are explicitly taken into account in the model. Each rotor speed is subject to physical saturation limits, which restrict the minimum and maximum achievable motor speeds. In addition, actuator faults are modeled using loss-of-effectiveness factors that reduce the actual rotor speeds relative to the commanded values. These faults degrade the thrust and torque generation capabilities of the quadrotor and introduce uncertainties into the system dynamics. Based on this physical description, the quadrotor dynamic model provides a foundation for the development of a payload-aware fractional-order fault-tolerant containment control scheme. The use of fractional-order operators allows the controller to capture memory effects and improve robustness in the presence of actuator faults, input saturation, payload variations, and communication delays, which are commonly encountered in multi-UAV containment scenarios. The coordinate convention adopted in this section is consistent with Figure 1. The inertial reference frame is defined such that the positive vertical axis follows the same direction used throughout the system model and simulation, ensuring consistency in the dynamic description.

As shown in Figure 12, the quadrotor dynamics are defined with respect to the inertial and body-fixed coordinate frames.

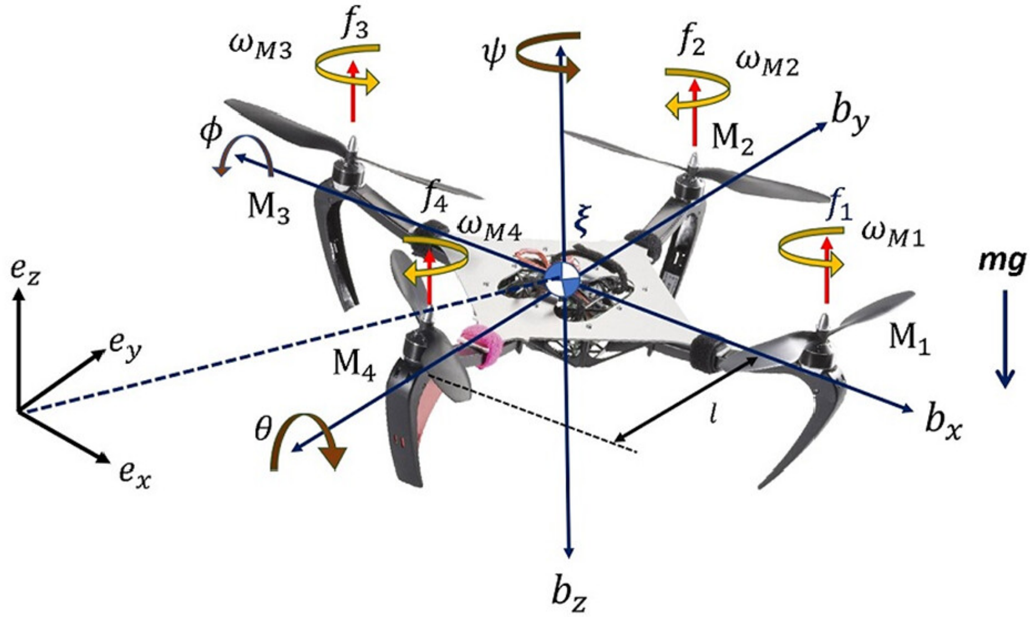

Figure 12. The inertial reference frame follows the North-East-Up (NEU) convention, where the positive z-axis points upward.

7. Conclusions

The problem of distributed containment tracking for fractional-order multi-drone networks subject to time-varying payloads, actuator degradation, input limits, and network latencies was resolved in this work. By introducing a payload-dependent state-space representation, the controller explicitly decoupled fractional dynamics from mass uncertainties. An online adaptive update mechanism was synthesized alongside this model to cancel out unmodeled payload fluctuations while strictly keeping control inputs within non-smooth saturation profiles.

Theoretical validation via fractional Lyapunov tools confirmed the admissibility of the entire closed-loop architecture, guaranteeing that all internal system states are uniformly bounded and that the containment errors asymptotically diminish to zero. Comprehensive numerical validation and algorithmic comparisons showcased the design's notable tracking fidelity and lowered control authority requirements relative to baseline methods. The main novelty of this work lies in the development of a unified adaptive fractional-order containment control framework that simultaneously addresses unknown time-varying payloads, actuator faults, input saturation, and communication delays. Unlike conventional containment control approaches, the proposed method combines online payload estimation with fractional-order sliding mode control to improve robustness and tracking accuracy under practical operating conditions. Theoretical analysis and simulation results demonstrate that the proposed framework delivers reliable containment performance while maintaining stability under multiple uncertainties. Although this work considers fixed actuator loss-of-effectiveness and bias fault models, practical UAV systems may experience abrupt, intermittent, or time-varying actuator faults. Extending the proposed adaptive containment control framework to accommodate these more complex fault characteristics will be an important direction for future research and practical implementation. Moving forward, the research line will focus on expanding these results to event-sampled communication, finite-time execution windows, cyber-physical defense protocols, and experimental physical deployment.

Author contributions

H. Louati: Conceptualization, software, formal analysis, supervision, project administration; M. M. A. Almazah: Validation, resources, data curation, writing original draft; H. Louati and M. M. A. Almazah: Writing-review and editing. All authors have read and approved the final version of the manuscript for publication.

Use of Generative-AI tools declaration

The authors declare they have not used Artificial Intelligence (AI) tools in the creation of this article.

Acknowledgments

The authors extend their appreciation to the Deanship of Research and Graduate Studies at King Khalid University for funding this work through the Large Research Project under grant number "RGP 2/26/47". The authors also express their appreciation to the Deanship of Scientific Research at Northern Border University, Arar, Saudi Arabia for funding this research work through project number "NBU - FPEJ - 2026 - 2920 - 01".

Code availability

The code is considered an intellectual property of King Khalid University Saudi Arabia, and is therefore not publicly available.

Data availability statement

The data that support the findings of this study are available from the corresponding author, Mohammad M.A. Almazah, upon reasonable request.

Conflict of interest

The authors declare that they have no conflict of interest.

References

1. Z. Yu, Y. Xu, Y. Zhang, B. Jiang, C. Y. Su, Fractional-order fault-tolerant containment control of multiple fixed-wing UAVs via disturbance observer and interval type-2 fuzzy neural network, *Int. J. Robust Nonlin.*, **33** (2023), 10257–10277. https://doi.org/10.1002/rnc.6577
2. B. Xian, S. Wang, S. Yang, Nonlinear adaptive control for an unmanned aerial payload transportation system: Theory and experimental validation, *Nonlinear Dynam.*, **98** (2019), 1745–1760. https://doi.org/10.1007/s11071-019-05283-0
3. B. Hichri, J. C. Fauroux, L. Adouane, I. Doroftei, Y. Mezouar, *Lifting mechanism for payload transport by collaborative mobile robots*, In: New Trends in Mechanism and Machine Science: From Fundamentals to Industrial Applications, Cham, Switzerland: Springer, 2014, 157–165.
4. S. Yang, B. Xian, Energy-based nonlinear adaptive control design for the quadrotor UAV system with a suspended payload, *IEEE T. Ind. Electron.*, **67** (2020), 2054–2064. https://doi.org/10.1109/TIE.2019.2902834
5. X. Liang, H. Yu, Z. Zhang, H. Liu, Y. Fang, J. Han, Unmanned aerial transportation system with flexible connection between the quadrotor and the payload: Modeling, controller design, and experimental validation, *IEEE T. Ind. Electron.*, **70** (2023), 1870–1882. https://doi.org/10.1109/TIE.2022.3163526
6. X. Liang, Y. Fang, N. Sun, H. Lin, X. Zhao, Adaptive nonlinear hierarchical control for a rotorcraft transporting a cable-suspended payload, *IEEE T. Syst. Man Cy.-S.*, **51** (2021), 4171–4182. https://doi.org/10.1109/TSMC.2019.2931812
7. P. Cheng, C. Cai, P. Park, Distributed event-triggered fractional-order fault-tolerant control of multi-UAVs with full-state constraints, *Nonlinear Dyn.*, **112** (2024), 1069–1085. https://doi.org/10.1007/s11071-023-09069-3
8. Y. Liu, Y. Dai, M. Li, L. He, Y. Chen, Distributed fuzzy formation control for networked UAVs with saturation constraints in resilient prescribed performance, *IEEE Internet Things J.*, 2025.
9. W. Li, L. Shi, M. Shi, J. Yue, B. Lin, K. Qin, Analyzing containment control performance for fractional-order multi-agent systems via a delay margin perspective, *IEEE Trans. Netw. Sci. Eng.*, **11** (2024), 2810–2821. https://doi.org/10.1109/TNSE.2024.3350122
10. X. Zhang, H. Pan, K. Ling, Enhanced robust association for multi-object tracking in multibeam forward-looking sonar video, *Ocean Eng.*, **350** (2026), 124141. https://doi.org/10.1016/j.oceaneng.2025.124141
11. N. Gu, C. Xu, C. An, Z. Chen, S. Chen, Unified aeroelastic and flight dynamics formulation based on state-space unsteady aerodynamics, *AIAA J.*, 2026, 1–18. https://doi.org/10.2514/1.J065498
12. C. Xie, L. Zhu, C. An, Y. Shao, A rapid steady/unsteady aerodynamic analysis method based on panel method coupled boundary layer theory, *Aerosp. Sci. Technol.*, **165** (2025), 110494. https://doi.org/10.1016/j.ast.2025.110494
13. Y. Tang, L. Dou, R. Zhang, X. Zhang, S. Cai, Adaptive dynamic programming-based fault-tolerant control of multi-UAV formation systems, *T. I. Meas. Control*, **47** (2025), 1893–1905. https://doi.org/10.1177/01423312241264070

14. Y. Hu, C. Bai, W. Wang, Z. Wang, Prior-controller-assisted multi-agent deep reinforcement learning attitude control for hypersonic morphing vehicles, *Aerosp. Sci. Technol.*, 2026. https://doi.org/10.1016/j.ast.2026.112803

15. M. Liu, W. Ma, C. Wang, P. Wang, M. Yang, Machine learning-enhanced rapid design of hydrodynamic shape for underwater vehicles pedigrees, *IEEE/ASME T. Mech.*, **31** (2025), 3107–3117. https://doi.org/10.1109/TMECH.2025.3639691

16. B. Zhong, H. Wang, Z. Lu, Y. Huang, J. Ren, Improved soft actor-critic for unmanned underwater vehicle obstacle avoidance, *IEEE T. Intel. Transp. Syst.*, **27** (2026), 9036–9050. https://doi.org/10.1109/TITS.2026.3698635

17. G. Cai, C. Huang, J. Feng, Y. Zhou, G. Yin, Real-time event-triggered tube MPC with ISS guarantees for vehicle motion control under disturbances, *IEEE/ASME T. Mech.*, 2026, 1–12. https://doi.org/10.1109/TMECH.2026.3695526

18. Z. Cai, Z. Fan, T. Liu, K. Kannaiyan, Neural network model for predicting aerodynamic parameters of airfoils, *J. Aircraft*, **63** (2025), 934–949. https://doi.org/10.2514/1.C038462

19. K. Hu, Z. Ma, S. Zou, J. Li, H. Ding, Impedance sliding-mode control based on stiffness scheduling for rehabilitation robot systems, *Cyborg Bionic Syst.*, **5** (2024). https://doi.org/10.34133/cbsystems.0099

20. B. Li, M. Chen, S. Qi, K. Peng, Finite-time fault-tolerant control of the attitude control system of a quadrotor UAV based on a neural network disturbance observer, *Neural Comput. Appl.*, **37** (2025), 5597–5606. https://doi.org/10.1007/s00521-024-10927-3

21. M. Lv, B. Zhang, H. Duan, Y. Shi, C. Zhou, *Specified-time fault-tolerant tracking control*, In: Unmanned Aerial Vehicles Formation Control and Safety Guarantee, Singapore: Springer, 2025, 93–122.

22. Q. Deng, Z. Li, J. Liu, S. Li, P. Luo, K. Cui, Data-driven modeling and control considering time delays for WPT systems, *IEEE T. Power Electron.*, **37** (2022), 9923–9932. https://doi.org/10.1109/TPEL.2022.3151941

23. Y. Tian, H. Tian, A multi-layer dynamic model of information propagation considering individual three-phase linear modulated behaviors, *Physica A*, **689** (2026), 131427. https://doi.org/10.1016/j.physa.2026.131427

24. W. Liang, X. Sun, Y. Ji, J. Wu, X. Liu, Anonymous dynamic formation control of multiagent systems with obstacle avoidance, *IEEE T. Reliab.*, **75** (2026), 1079–1093. https://doi.org/10.1109/TR.2026.3665586

25. T. Wang, Z. Zhu, X. Zhou, T. Jing, W. Chen, A function-based behavioral modeling method for air combat simulation, *J. Syst. Eng. Electron.*, **35** (2024), 945–954. https://doi.org/10.23919/JSEE.2024.000068

26. H. Zhong, H. Zhang, S. Zhen, H. Sun, X. Chen, X. Liu, et al., Adaptive robust control for underactuated bipedal parallel wheel-legged robots: A Nash game-based constraint following approach, *IEEE T. Fuzzy Syst.*, **34** (2026), 1791–1803. https://doi.org/10.1109/TFUZZ.2026.3670620

27. S. Zhen, W. Ye, X. Liu, A leakage-type adaptive robust control method for collaborative robot joints with fuzzy uncertainty: Trajectory constraints and parameter optimization, *Inform. Sci.*, **754** (2026), 123674. https://doi.org/10.1016/j.ins.2026.123674
28. Q. Li, Q. Huang, W. Jiang, Z. Song, X. Wu, Hands-free mobility control: A low-latency asynchronous MI-BCI system for real-time robotic navigation with cognitive-ergonomic enhancement, *IEEE T. Human-Mach. Syst.*, **56** (2026), 291–300. https://doi.org/10.1109/THMS.2026.3659708
29. C. Wen, G. Chen, X. Gu, W. Wang, Joint optimization of communication rates for multi-UAV relay systems, *Complex Intell. Syst.*, **11** (2025). https://doi.org/10.1007/s40747-025-01910-z
30. P. Yang, A. Zhang, D. Zhou, Event-triggered finite-time formation control for multiple unmanned aerial vehicles with input saturation, *Int. J. Control Autom. Syst.*, **19** (2021), 1760–1773. https://doi.org/10.1007/s12555-019-0833-7
31. W. Y. H. Adoni, S. Lorenz, J. S. Fareedh, R. Gloaguen, M. Bussmann, Investigation of autonomous multi-UAV systems for target detection in distributed environments: Current developments and open challenges, *Drones*, **7** (2023). https://doi.org/10.3390/drones7040263
32. C. Su, J. Yuan, E. Zheng, W. Xu, Z. Liu, J. Hu, CPFL: Resilient continuous UAV localization via cross-view perception and particle filtering, *Drones*, **10** (2026). https://doi.org/10.3390/drones10060437
33. X. Tang, Q. Chen, W. Weng, C. Jin, Z. Liu, J. Wang, et al., Task assignment and exploration optimization for low-altitude UAV rescue via generative AI-enhanced multi-agent reinforcement learning, *IEEE T. Mobile Comput.*, **25** (2026), 627–643. https://doi.org/10.1109/TMC.2025.3594188
34. H. Tang, C. Bai, J. Guo, HAPPD: Cooperative pursuit strategy for fixed-wing UAVs in complex terrain, *IEEE T. Autom. Sci. Eng.*, **23** (2026), 9076–9091. https://doi.org/10.1109/TASE.2026.3689719
35. Y. Fu, B. Wang, H. Zhao, M. Zhou, N. Li, Z. Gao, Adaptive safety attitude control of a hybrid VTOL UAV under transition flight subject to multiple faults and uncertainties, *Aerosp. Sci. Technol.*, **163** (2025). https://doi.org/10.1016/j.ast.2025.110284
36. M. Benaissa, E. H. Al-Sabri, M. Iqbal, W. Abdelfattah, G. A. Alsawah, A. U. K. Niazi, Output formation containment of time-delayed heterogeneous singular multi-agent systems with stochastic impulsive effects, *AIMS Math.*, **11** (2026), 11706–11730. https://doi.org/10.3934/math.2026482
37. A. Alsinai, I. Al-Hejri, A. U. K. Niazi, M. Iqbal, A. Smerat, Robust bipartite containment control of multi-agent systems under stochastic disturbances and false data injection attacks via zero-sum game strategy, *J. Appl. Comput. Mech.*, 2025. https://doi.org/10.22055/jacm.2025.48738.5461
38. A. Alsinai, A. U. K. Niazi, M. Iqbal, A. Smerat, Consensus control of fractional-order singular multi-agent systems via adaptive pinning under switching topologies, *Int. J. Optim. Control Theor. Appl.*, **16** (2026), 349–369. https://doi.org/10.36922/IJOCTA025280123
39. X. Zhan, X. Du, J. Wu, H. Yan, Performance analysis of MIMO information time-delay systems with message queues under multiple communication parameters, *IEEE Trans. Syst., Man Cyb.-S.*, **54** (2024), 88–96. https://doi.org/10.1109/TSMC.2023.3304310

40. L. Ma, F. Zhu, Predefined-time synchronized bipartite formation control for networked heterogeneous Euler–Lagrange systems, *Math. Comput. Simul.*, **247** (2026), 705–721. https://doi.org/10.1016/j.matcom.2026.03.038

41. X. Chen, L. Ma, X. Zhao, G. Zong, Predefined-time sliding-mode formation control for second-order nonlinear multi-agent systems under deception attacks, *Eur. J. Control*, 2026. https://doi.org/10.1016/j.ejcon.2026.101534

42. J. Chen, C. Yu, Y. Wang, Z. Zhou, Z. Liu, Hybrid modeling for vehicle lateral dynamics via AGRU with a dual-attention mechanism under limited data, *Control Eng. Pract.*, **151** (2024). https://doi.org/10.1016/j.conengprac.2024.106015

43. D. Li, S. Tong, H. Yang, Q. Hu, Time-synchronized control for spacecraft reorientation with time-varying constraints, *IEEE/ASME T. Mech.*, **30** (2025), 2073–2083. https://doi.org/10.1109/TMECH.2024.3430953

44. Z. Zhou, Y. Wang, X. Liu, Z. Li, M. Wu, G. Zhou, Hybrid of neural network and physics-based estimator for vehicle longitudinal dynamics modeling using limited driving data, *IEEE T. Intel. Transp. Syst.*, **26** (2025), 16735–16746. https://doi.org/10.1109/TITS.2025.3585346

45. J. Chen, M. Li, M. Marcantoni, B. Jayawardhana, Y. Wang, Range-only distributed safety-critical formation control based on contracting bearing estimators and control barrier functions, *IEEE Internet Things J.*, **12** (2025), 40968–40979. https://doi.org/10.1109/JIOT.2025.3590774

46. W. Guo, J. Liu, W. Qin, X. Lan, H. Bai, X. Li, Robust adaptive dynamic programming for morphing air-breathing hypersonic vehicles under unmatched uncertainty, *Sci. China Inform. Sci.*, **69** (2026). https://doi.org/10.1007/s11432-024-4386-4

47. R. Li, J. Jin, D. Zhang, C. Chen, A segmented activation function-based zeroing neural network model for dynamic Sylvester equation solving and robotic manipulator control, *Concurr. Comp.-Pract. E.*, **37** (2025). https://doi.org/10.1002/cpe.70243

48. J. Xiong, X. Wang, Adaptive sliding mode control for uncertain tilting quadrotors using randomized feedforward neural networks, *Int. J. Robust Nonlin. Control*, **36** (2026), 4042–4055. https://doi.org/10.1002/rnc.70396

49. J. Zhang, C. P. Tan, G. Zheng, Y. Wang, On sliding mode observers for non-infinitely observable descriptor systems, *Automatica*, **147** (2023), 110676. https://doi.org/10.1016/j.automatica.2022.110676

50. Q. Wang, J. Cao, H. Liu, Adaptive fuzzy control of nonlinear systems with predefined time and accuracy, *IEEE T. Fuzzy Syst.*, **30** (2022), 5152–5165. https://doi.org/10.1109/TFUZZ.2022.3169852

51. X. Yang, X. Zhang, J. Cao, H. Liu, Observer-based adaptive fuzzy fractional backstepping consensus control of uncertain multi-agent systems via event-triggered scheme, *IEEE T. Fuzzy Syst.*, **32** (2024), 3953–3967. https://doi.org/10.1109/TFUZZ.2024.3386312

52. M. Hou, J. Zhao, J. Tian, H. Du, Minimum operator-based data-driven sliding mode control for a magnetorheological fluid dual clutch, *IEEE T. Cyb.*, **55** (2025), 4991–5001. https://doi.org/10.1109/TCYB.2025.3596063

53. Z. Wang, X. Liu, X. Sun, P. Qi, S. Wu, A modified super-twisting sliding mode control for aircraft braking system with adaptive gain schedule and disturbance compensation, *IEEE T. Ind. Electron.*, **73** (2026), 4308–4318. https://doi.org/10.1109/TIE.2025.3613654

54. X. Liu, X. Sun, Z. Wang, N. Bai, Y. Shang, Adaptive aircraft anti-skid braking control for runway disturbance compensation, *Control Eng. Pract.*, **159** (2025), 106314. https://doi.org/10.1016/j.conengprac.2025.106314

55. J. Zhao, D. Xu, X. Zhang, X. Li, Inverse optimal tracking control for AC/DC converter based on inverse reinforcement learning, *Int. J. Control Autom. Syst.*, **24** (2026), 320–331. https://doi.org/10.1007/s12555-026-00015-8

56. B. Feng, Z. Wang, L. Yuan, Q. Zhou, Y. Chen, Y. Bi, Towards safe motion planning for industrial human-robot interaction: A co-evolution approach based on human digital twin and mixed reality, *Robot. Compu.-Int. Manuf.*, **95** (2025), 103012. https://doi.org/10.1016/j.rcim.2025.103012